Journal of Electrical and Electronic Engineering
2022; 10(1): 1-9
http://www.sciencepublishinggroup.com/j/jeee
doi: 10.11648/j.jeee.20221001.11
ISSN: 2329-1613 (Print); ISSN: 2329-1605 (Online)

Electron Density Estimation and Fiber Fuse Simulation in Laser-Irradiated Bulk Glass

Yoshito Shuto

Ofra Project, Iruma, Japan

Email address:
ofra@tuba.ocn.ne.jp

To cite this article:
Yoshito Shuto. Electron Density Estimation and Fiber Fuse Simulation in Laser-Irradiated Bulk Glass. *Journal of Electrical and Electronic Engineering*. Vol. 10, No. 1, 2022, pp. 1-9. doi: 10.11648/j.jeee.20221001.11

Received: December 26, 2021; **Accepted**: January 11, 2022; **Published**: January 18, 2022

Abstract: To clarify the formation mechanism of periodic nanometer-size cavity structure of a borosilicate glass sample, the free electron density around the exit surface was investigated when it exposed to intense femtosecond laser radiation. The electron density near the edge of the crack on the surface was estimated to be 10^{20}-10^{22} cm^{-3}. From this result, the temperature of the irradiated heating area near the edge of the crack was estimated to reach at least about 6,000 K, which was sufficient for the initiation and propagation of the fiber fuse. In this way, periodic nanosized cavities could be formed by fiber fuse propagation starting near the edge of the crack on the exit surface. Next, fiber fuse propagation in the modified zone formed by continuous-wave laser irradiation in a silica glass sample was investigated theoretically by the explicit finite-difference method using the thermochemical SiO_x production model. In the calculation, we assumed the glass to be in an atmosphere and that part (40 μm in length) of the modified zone was heated to a temperature of 2,923 K. The calculated velocities of fiber fuse propagation in the modified zone were in fair agreement with the experimental values observed at 0.514 and 1.064 μm.

Keywords: Bulk Glass, Fiber Fuse Phenomenon, Finite-difference Technique

1. Introduction

Ultrashort laser pulses can be used to rapidly and precisely deposit energy in transparent materials. 3D integrated photonics [1] and Ultrashort-laser-inscribed 3D optical data strage [2] are proposed. Femtosecond (fs) laser inscription technique has been applied to independent core attenuation control in multicore fibers [3] and reduction of differential mode gain in a two-mode erbium-doped fiber [4].

The ultrashort laser pulses are absorbed by electrons, and the optical excitation ends before the lattice is perturbed. It takes picoseconds for the electrons to transfer their excess energy to the lattice, and nanoseconds for micrometer-scale atomic displacement to occur [5]. Energy from the ultrashort laser pulse is coupled into the material through a combination of multiphoton absorption and avalanche ionization [6-14].

When an fs laser pulse is focused inside the bulk of a transparent material as shown in Figure 1 (a), the intensity in the focused region can become high enough to cause absorption through nonlinear processes, leading to optical breakdown in the material. The ultrafast energy deposition creates high temperature and pressures inside the focused region and the material is ejected from the center and forced into the surrounding volume, leading to the formation of a structure consisting of a cavity (or at least of less dense material) with a submicrometer diameter surrounding by densified material [1]. By using an fs laser with a high repetition rate, it is possible to write waveguides, where laser damage spots are continuously formed in the glass [15-17].

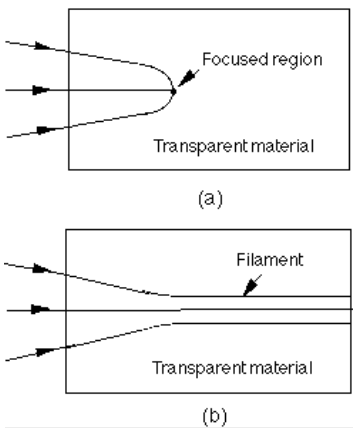

Figure 1. *Focusing and filamentation in transparent material.*

In contrast, the formation of a self-guided filament over a long distance (at least 1 mm) upon irradiation with a focused fs laser beam inside the fused silica was reported by several research institutes [18-23] (see Figure 1 (b)). A filament results from the dynamic competition between the self-focusing and defocusing of electron plasma at powers around the critical value of self-focusing [21, 23].

One of the problems arising from high power injection in the silica glass is the probability of detonating the fiber fuse effect. This phenomenon was discovered by British researchers in 1987-1988 in conventional single-mode optical fibers [24-28]. Recently, the occurrence of fiber fuse in bulk glasses [18, 19, 29-33] has been reported.

In this article, we describe the fiber fuse phenomenon observed in bulk glasses.

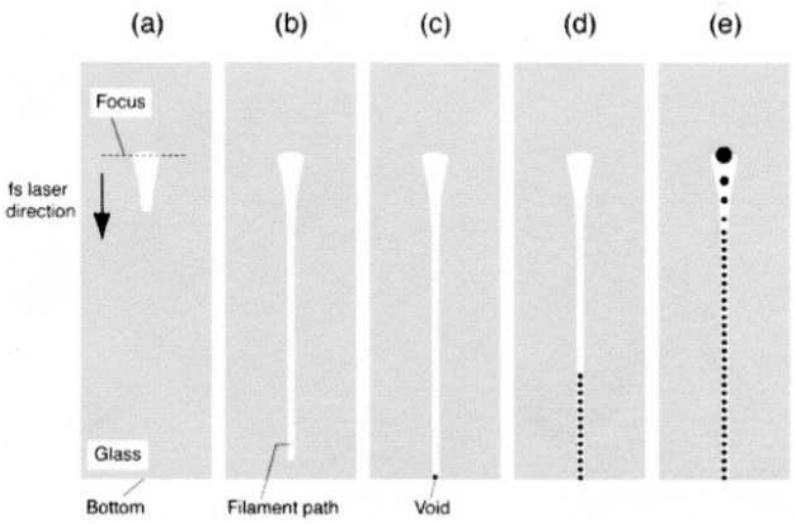

Figure 2. *Schematic illustration for the formation process of the periodic cavities [18].*

2. Electron Density in Bulk Glass Irradiated by Ultrashort Laser Pulses

Recently, Kanehira *et al.* observed the occurrence of periodic cavities in a self-guided filament [18, 19]. A regeneratively amplified 0.8 μm Ti: sapphire laser that emits 120 fs, 1 kHz, mode-locked pulses was used in their experiments. Launching a focused fs laser beam into a conventional borosilicate glass sample induces a change in the refractive index at the focal point, as shown in Figure 2 (a), and then a self-guided filament path propagates toward the bottom surface of the glass sample, as shown in Figure 2 (b).

Once the core of the filament line is raised to a sufficiently high temperature, it becomes highly absorbent as described in [34-36].

When the self-guided filament reaches the edge of the glass sample, optical breakdown (or microexplosion) occurs around the bottom surface to create a nanosized void (cavity), as shown in Figure 2 (c). When the next fs laser pulse propagates from the focal point, it is trapped in the heated region around the cavity formed beforehand, resulting in the production of a new high temperature region and the formation of the next cavity. The region that absorbs the laser light thus moves to a new point along the filament path, and the process is repeated many times, as shown in Figure 2 (d). In this manner, the fiber fuse is generated and propagates in the glass sample. The fuse propagates along the self-guided filament path toward the laser source, becoming larger close to the focal point, as shown in Figure 2 (e).

The cavity size (l) and period (Λ) was 0.6 μm and 1.6 μm, respectively, when the pulse energy was 10 μJ for 1 s. These values increased to be 1.0 μm and 3.2 μm, respectively, when the pulse energy increased from 10 μJ to 40 μJ for 1 s. From these data, it is clear that the l / Λ value of the cavity decreased from 0.375 to 0.3125 with increasing the pulse energy.

In order to initiate the fiber fuse, a high temperature of 2,900 K and above is needed [36] at the nanosized void in the bottom surface. Here we consider the response of the borosilicate glass material in [18, 19] to the laser excitation around the bottom surface. The peak power of the laser pulse is about 83 kW when the pulse energy was 10 μJ for 1 s. When this large power was concentrated on a small area around the bottom surface, the laser pulse created a hot, high-density electron plasma [5]. The plasma transfers its excess energy to the lattice and heats it before the energy escapes by diffusion on a time scale of < 10 ps.

Stuart *et al.* derived the following simple rate equation for the evolution of the free electron density N_e in a dielectric medium exposed to intense laser radiation [8, 9, 11]:

$$\frac{\partial N_e}{\partial t} = \alpha I(t) N_e + \alpha_k I^k(t) \qquad (1)$$

where $I(t)$ is the intensity of the laser pulse, α is the avalanche coefficient, and α_k is the k-photon absorption cross section with the smallest k satisfying $k\hbar\omega \geq E_g$ (E_g is the band-gap energy of the material).

For the borosilicate glass material, values of $E_g \sim 4$ eV, $\alpha = (1.2 \pm 0.4)$ cm^2/J, and $\alpha_3 = 7 \times 10^{17\pm0.5}$ cm^{-3} ps^{-1} (cm^2/TW)^3 at a

wavelength (λ_0) of 0.78 μm were reported by Lenzner *et al.* [11]. If we assume that the diameter of the irradiated area is 2 μm, the peak intensity of the 120 fs pulse becomes 2.65 TW/cm^2 when the pulse energy is 10 μJ for 1 s.

Figure 3 shows the evolution of electron density for this pulse. Because multiphoton ionization is strongly intensity dependent, electrons are mainly produced near the peak of the pulse and N_e reaches about 1.2 × 10^{18} cm^{-3} after the passage of the pulse. N_e of 10^{18} cm^{-3} order was observed at a temperature of about 5,000 K in silica glass [37]. Therefore, the temperature of the irradiated heating area will reach about 5,000 K and above, which was sufficient for the initiation and propagation of the fiber fuse [26].

Why does a nanosized void occur at the surface of the glass sample? It has been observed that surfaces generally have a lower threshold for damage than the bulk material [38-42].

When a light pulse enters a glass sample at near-normal incidence, as shown in Figure 4, the electric field strength E_{bulk} of the light pulse transmitted through the sample is given by [41]

$$E_{bulk} = [2/(n+1)]\, E_0 \quad (2)$$

where n (= 1.5) is the refractive index of the glass sample and E_0 is the electric field strength of the incident light pulse. When this transmitted light pulse exits the sample, the electric field strength E_{exit} at the exit surface is given by [41]

$$E_{exit} = [2n/(n+1)]\, E_{bulk} = [4n/(n+1)^2]\, E_0 \quad (3)$$

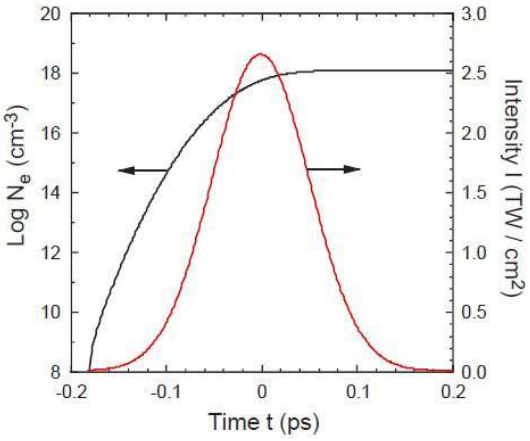

Figure 3. *Calculated evolution of free electron density N_e for a 120 fs pulse (red curve) of peak intensity of 2.65 TW/cm^2 in a borosilicate glass sample.*

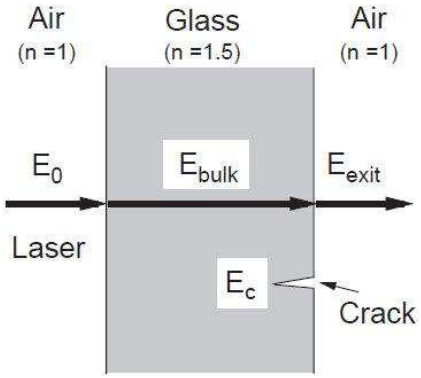

Figure 4. *Schematic illustration of laser pulse transmission in a glass sample.*

Thus, the nominal breakdown intensity of the light pulse at the exit surface is lower by a factor of $4n^2 / (n+1)^2$ (= 1.44) than that of the bulk. This factor is called the light intensity enhancement factor (LIEF) [43].

The ideas concerning the importance of the electric field strength at the surface of a dielectric material were extended by Bloembergen to investigate the role of submicroscopic cracks and pores in surface damage [44, 45].

If the crack shown in Figure 4 is mathematically represented by a disk-shaped ellipsoidal void (or conical crack), with the lines of forces in the bulk normal to the disk, the electric field will be concentrated near the edge, increasing the electric field strength by a factor of n^2. That is, the electric field strength E$_c$ near the edge of the crack is given by [45]

$$E_C = n^2\, E_{bulk} \quad (4)$$

Consequently, the breakdown intensity of the light pulse at this location on the exit surface is lower by an LIEF of n^4 (= 5.06) than that of the bulk. Furthermore, Génin *et al.* numerically calculated LIEF values owing to conical surface cracks [43]. They found that the LIEF value can locally reach two orders of magnitude that for conical cracks of ideal shape and theoretical LIEF values for the conical cracks range from 5 to 102 [43].

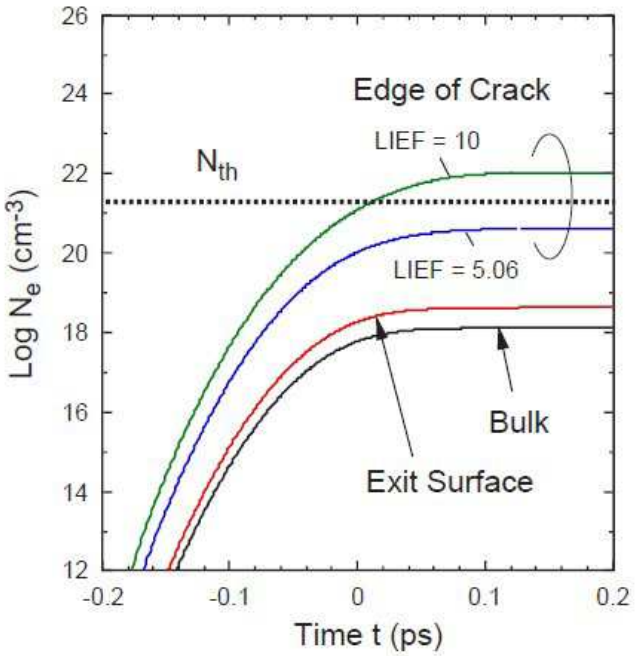

Figure 5. *Calculated evolution of free electron densities for a 120 fs pulse of peak intensity of 2.65 TW/cm^2 in the bulk, at the exit surface, and near the edge of the crack of a borosilicate glass sample.*

Figure 5 shows the evolution of electron densities for a 120 fs pulse of peak intensity of 2.65 TW/cm^2 in the bulk, at the exit surface, and near the edge of the crack forming on the exit surface. The LIEF values of 5.06 and 10 were assumed for the crack. N_{th} ($\cong 2 \times 10^{21}$ cm^{-3} [6, 21]) is the plasma critical density. The N_e value at the exit surface reaches about 3.9 × 10^{18} cm^{-3} after the passage of the pulse, which is about three times that in the bulk. On the other hand, N_e near the edge of the crack

reaches about 3.7×10^{20} cm^{-3} in the case of LIEF = 5.06. This value is about 300 times larger than that in the bulk and is one order of magnitude below the plasma critical density N_{th}. N_e of 10^{20} cm^{-3} order was observed at a temperature of about 6,000-7,000 K in the silica glass [37]. Therefore, the temperature of the irradiated heating area near the edge of the crack will reach at least about 6,000 K.

If a value of LIEF = 10 is assumed for the cracks on the exit surface, N_e near the edge of the crack reaches about 1×10^{22} cm^{-3} as shown in Figure 5. As this value is larger than the N_{th} ($\cong 2 \times 10^{21}$ cm^{-3}), laser light is strongly absorbed, leading to rapid heating of the electron plasma. As a result, laser-induced breakdown (or a microexplosion) occurs near the edge of the crack on the bottom (exit) surface and a dense plasma is formed in the bulk around the bottom surface, which results in the nanosized cavity as shown in Figure 2 (c).

The irradiated heating area near the bottom surface is considered to be thermodynamically unstable owing to the large increment ($\geq$ 5,000 K) of the local temperature. As described in [46], thermodynamic instability results in a decrease in the l / Λ value of the cavity. From the experimental results with respect to the l / Λ values described above, it can be considered that the cavity formation process in the self-guided filament is thermodynamically unstable and the instability of the process increases with increasing the pulse energy of a focused fs laser beam.

3. Fiber Fuse Effect in Bulk Glass

3.1. Modified Zone Formed by CW Laser Irradiation

Hidai *et al.* observed the occurrence of periodic cavities in bulk glass by irradiation of a continuous-wave (CW) laser beam [29-32]. A schematic illustration of their experimental setup is shown in Figure 6. Thin copper foil, serving as an absorbent, was placed on the borosilicate glass.

Another glass plate and a weight were placed on the metal foil to ensure good contact between the glass sample and the absorbent (metal foil). A CW laser beam (Ar ion laser) operating at $\lambda_0 = 0.514$ μm was focused on the metal foil. The spot diameter of the laser beam in air was approximately 53 μm. When the refractive index of glass was considered, the estimated diameter of the focal spot in the glass was ~36 μm [31]. After the start of laser irradiation, bright emission was observed at the interface of the glass sample and the absorbent, and then the emission moved toward the light source. The modified zone was formed after passage of the emission through the glass sample. The width (or diameter) of the modified zone in silica glass was about 60 μm [29]. After the laser exposure, a periodic structure of cavities was observed at the center of the modified zone near the upper surface (in contact with the absorbent) of the glass sample. The cavity size (l) and period (Λ) in silica glass were 15 μm and 52 μm, respectively, when the laser power (P_0) was 11 W (see Figure 3 in [31]). The l / Λ value was 0.288 near the upper surface and increased to be about 0.5 around the middle (~3 mm from the upper surface), and became 1 at the tip (~5.5 mm from the upper surface) of the glass sample. At the tip, a long filament was observed. No cavities and/or filaments were found in other parts of the glass sample.

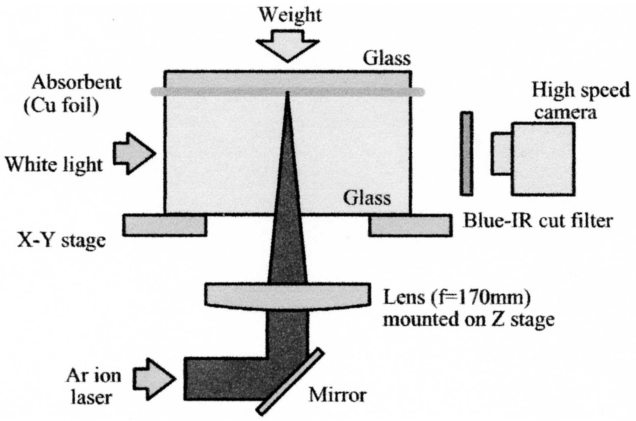

Figure 6. *Schematic illustration of experimental setup used by Hidai et al. [30].*

The mechanism causing the periodic cavities was explained as follows. When the laser beam was focused on the absorbent, the temperature of the laser-illuminated spot on the absorbent increased. The optical absorption coefficient α is related to the extinction coefficient k and λ_0 by [47]

$$\alpha = 4\pi k / \lambda_0 \tag{5}$$

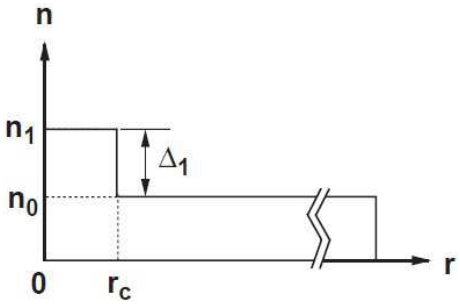

Figure 7. *Refractive-index profile of the silica glass sample.*

A value of $k = 2.42$ for copper at $\lambda_0 = 0.50$ μm has been reported [48]. Using Eq. (5) and this k value, the absorption coefficient of copper is estimated to be $\alpha = 5.92 \times 10^7$ m^{-1} at $\lambda_0 = 0.514$ μm. This value is about three orders of magnitude larger than the α value (10^4 m^{-1} order) required for fiber fuse generation.

The part of the glass sample in contact with the heated absorbent was also heated by thermal conduction and radiation from the absorbent, as described in [49]. Then this part started to absorb the laser beam because of its enhanced absorption owing to the temperature rise. The heated part of the sample also heated the surrounding area, which also started to absorb the laser beam. By repeating this process, the heated spot moved backward (toward the light source) until it reached the point where the fluence was insufficient to heat the glass because of defocusing. The modified zone was formed by heating and quenching.

The modification speed, which corresponds to the fiber fuse propagation velocity V_f, was about 200 mm/s when the input

laser power (P_0) was 10 W and increased with increasing P_0 [32]. The laser fluence at the focus, which corresponds to the threshold power density I_{th}, was about 1 MW/cm^2 [31]. This value is the same magnitude of the I_{th} value observed in the fiber fuse experiments [50]. Therefore, it is considered that the migration of the bright spot observed by Hidai *et al.* [29-32] occurs by the same mechanism as that of the fiber fuse phenomenon.

3.2. Fiber Fuse Calculation in Silica Glass at 0.514 μm

We investigated the generation of a fiber fuse and its propagation in the modified zone by the explicit finite-difference method.

The refractive-index profile of the silica glass sample, in which the modified zone is formed, is shown in Figure 7. In this figure, r_c is the radius of the modified zone, and n_1 and n_0 are the refractive indices of the modified zone and the silica glass, respectively. The relative refractive-index difference Δ_1 between n_1 and n_0 is defined as

$$\Delta_1 = \frac{(n_1^2 - n_0^2)}{2n_1^2} \sim (n_1 - n_0)/n_1 \quad (6)$$

In the calculation, we assumed n_1 = 1.46187, n_0 = 1.46181, and Δ_1 = 0.004% at λ_0 = 0.514 μm. These refractive indices were estimated using the Sellmeier equation described in [51].

We assumed the glass to be in an atmosphere with temperature $T = T_a$. We also assumed that part of the modified zone\index{modified zone} of length ΔL is heated to a temperature of T^0_c (> T_a), as shown in Figure 8. In the heating zone (called the "hot zone") shown in Figure 8, the optical absorption coefficient α is larger than in other parts of the modified zone because of its high temperature T^0_c (> T_a).

Thus, as light propagates along the positive direction (away from the light source) in this zone, a considerable amount of heat is produced by light absorption.

The calculation by the finite-difference method followed the procedure described in the literature [34-36]. In the calculation, we set r_c to 18 μm, the time interval δt to 1 ns, the step size along the r axis δr to 5 μm, and the step size along the z axis δz to 20 μm, and assumed that ΔL = 40 μm, T^0_c = 2,923 K and T_a = 298 K.

We estimated the temperature field T (r, z) near the modified zones at t = 1 ms and 11 ms after the incidence of laser light with P_0 = 10 W and λ_0 = 0.514 μm. The calculated temperature fields are shown in Figures 9 and 10. As shown in Figure 9, the core center temperature near the end of the hot zone (z = -0.16 mm) changes abruptly to a high value of about 19 × 10^4 K after 1 ms. This rapid rise in the temperature initiates the fiber fuse propagation, as shown in Figure 10. After 11 ms, the high-temperature front in the core layer reaches a z value of -2.12 mm. The average propagation velocity V_f is estimated to be 196 mm/s using these data. This V_f is close to the value (~200 mm/s) measured by Itoh *et al.* [32].

Furthermore, the P_0 dependence of the V_f values for the modified zone was examined at λ_0 = 0.514 μm. The calculated results are shown in Figure 11. The data reported by both Itoh *et al.* [32] are plotted in this figure. As shown in Figure 11, the V_f values estimated at λ_0 = 0.514 μm agree well with the experimental values.

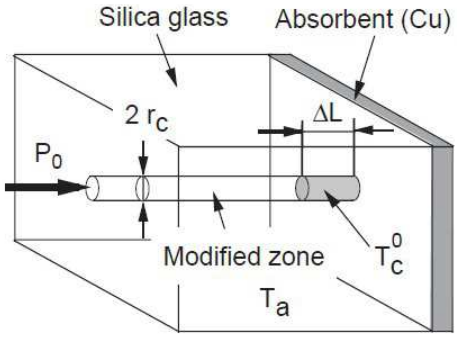

Figure 8. *Hot zone in silica glass sample.*

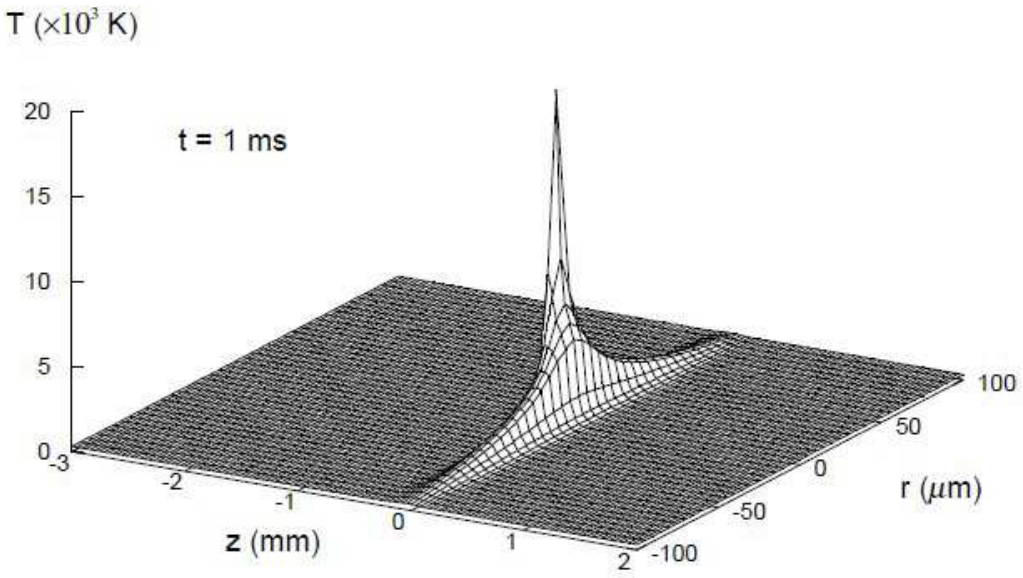

Figure 9. *Temperature field near the modified zone after 1 ms when P_0 = 10 W at λ_0 = 0.514 μm.*

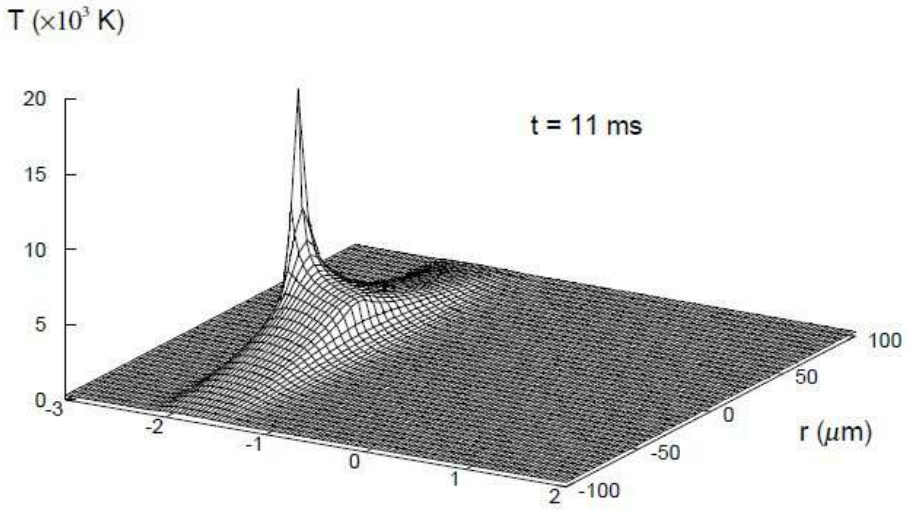

Figure 10. *Temperature field near the modified zone after 11 ms when P_0 = 10 W at λ_0 = 0.514 μm.*

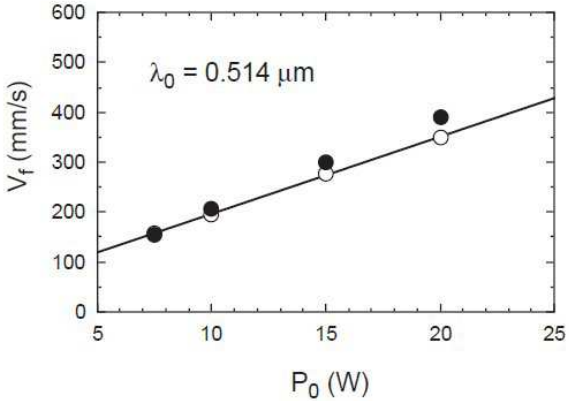

Figure 11. *Relationship between the velocity V_f and the input power P_0 at λ_0 = 0.514 μm. The open circles are the calculated results. The closed circles are the data reported by Itoh et al. [32].*

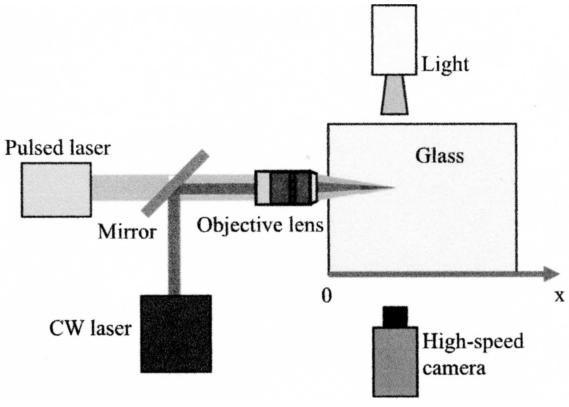

Figure 12. *Schematic illustration of experimental setup used by Tokunaga et al. [33].*

3.3. Modified Zone Formed by Pulsed and CW Laser Irradiation

Recently, Tokunaga *et al.* proposed a novel method of triggering a fiber fuse inside a bulk glass sample without requiring the use of metal foil as an absorbent [33]. A schematic illustration of their experimental setup is shown in Figure 12. Two types of laser were used in their method. One was the second harmonic of a nanosecond (ns)-pulsed Nd:YAG laser with λ_0 = 0.532 μm and pulse width of 3--5 ns. The repetition rate and the pulse energy of the pulsed laser were 10 Hz and 1.8 mJ, respectively. The other one was a CW Nd:YAG laser with λ_0 = 1.064 μm and P_0 = 50 W. In their method, optical breakdown by irradiation of ns laser pulses was utilized to initiate the fiber fuse. If we assume that the diameter of the irradiated area is about 4.2 μm, the peak intensity of the 5 ns pulse becomes 260 GW/cm^2 when the ns pulse energy is 1.8 mJ for 1 s. This is close to the intrinsic damage limit for silica, which exceeds 100 GW/cm^2 [52].

For pulses longer than a few tens of picoseconds, the generally accepted picture of bulk damage to defect-free dielectrics involves the heating of conduction band electrons by the incident radiation and transfer of this energy to the lattice. Damage (or breakdown) occurs through conventional heat deposition (heating of the lattice) resulting in the melting and boiling of the dielectric material [7, 9]. The breakdown region, which is the focal point of the pulsed laser, started to absorb the CW laser light, causing the temperature increase in the vicinity.

The high temperatures generated at the focal point caused the fiber fuse phenomenon. The bright spot propagated along the modified zone toward the laser source until it reached the glass surface. In addition, a long hole was drilled on the light source side of the glass.

The migration speed of the bright spot, which corresponds to the V_f, and the power density I were estimated to be 430 mm/s and 2.2 MW/cm^2, respectively, when the input CW laser power (P_0) was 50 W at λ_0 = 1.064 μm. These V_f and I values are similar to those (480 mm/s and 3.1 MW/cm^2) of an SMF-28 fiber observed in fiber fuse experiments [50]. Therefore, it can be concluded that the migration of the bright spot observed by Tokunaga *et al.* [33] occurs by the same mechanism as that of the fiber fuse phenomenon.

3.4. Fiber Fuse Calculation in Silica Glass at 1.064 μm

We investigated the generation of a fiber fuse and its propagation in the modified zone by the explicit

finite-difference method. In the calculation, we assumed n_1 = 1.45010, n_0 = 1.44988, and Δ_1 = 0.015% at λ_0 = 1.064 μm.

We assumed the silica glass to be in an atmosphere with temperature $T = T_a$. We also assumed that part of the modified zone of length ΔL is heated to a temperature of T^0_c ($> T_a$), as shown in Figure 13.

In the calculation, we set r_c to 27 μm, the time interval δt to 1 ns, the step size along the r axis δr to 5 μm, and the step size along the z axis δz to 20 μm, and assumed that ΔL = 40 μm, T^0_c = 2,923 K and T_a = 298 K. We estimated the temperature field $T(r, z)$ near the modified zones at t = 1 ms and 11 ms after the incidence of laser light with P_0 = 50 W and λ_0 = 1.064 μm.

The calculated temperature fields are shown in Figures 14 and 15. As shown in Figure 14, the core center temperature near the end of the hot zone (z = -0.40 mm) changes abruptly to a high value of about 4.0 × 10^4 K after 1 ms. This rapid rise in the temperature initiates the fiber fuse propagation, as shown in Figure 15. After 11 ms, the high-temperature front in the core layer reaches a z value of -4.56 mm. The average propagation velocity V_f is estimated to be 416 mm/s using these data. This V_f is close to the value (~430 mm/s) measured by Tokunaga *et al.* [33].

4. Conclusion

The formation mechanism of periodic nanometer-size cavity structure of a borosilicate glass sample was clarified by estimating the free electron density around the exit surface when the glass was exposed to intense femtosecond laser radiation. The electron density near the edge of the crack on the surface was estimated to be 10^{20}-10^{22} cm^{-3}.

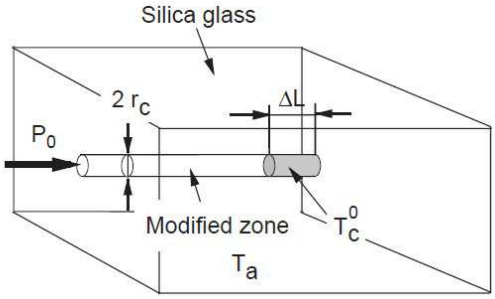

Figure 13. *Hot zone in the silica glass sample without metal absorbent.*

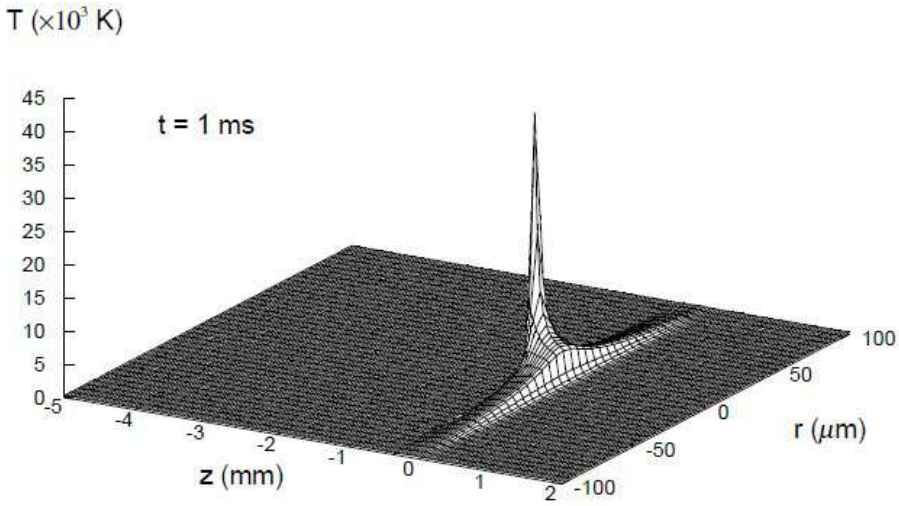

Figure 14. *Temperature field near the modified zone after 1 ms when P_0 = 50 W at λ_0 = 1.064 μm.*

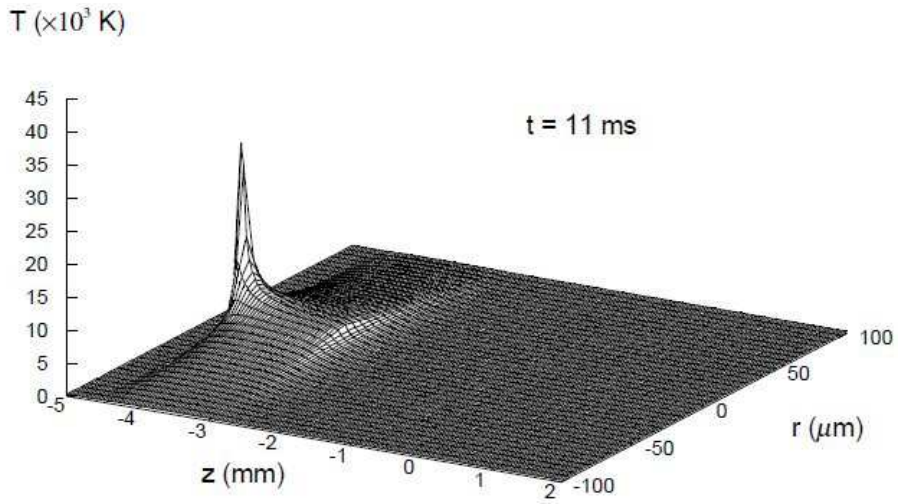

Figure 15. *Temperature field near the modified zone after 11 ms when P_0 = 50 W at λ_0 = 1.064 μm.*

From this result, it was found that periodic nanosized cavities could be formed by fiber fuse propagation starting near the edge of the crack on the exit surface. Next, the unsteady-state thermal conduction process in a modified zone formed by continuous-wave laser irradiation in a silica glass sample was studied theoretically by the explicit finite-difference method using the thermochemical SiO_x production model. The calculated velocities of fiber fuse propagation in the modified zone were in fair agreement with the experimental values.

References

[1] Gross S. and Withford M. J. (2015). Ultrafast-laser-inscribed 3D integrated photonics: challenges and emerging applications. Nanophotonics, 2015 (4), 332-352.

[2] Glezer E. N., Milosavljevic M., Huang L., Finlay R. J., Her T. H., Callan J. P., and Mazur E. (1996). Three-dimensional optical strage inside transparent materials. Opt. Lett., 21 (24), 2023-2025.

[3] Beresna M., Jung Y., Wang Y., Hayes J., Alam S. U., Brambilla G., and Richardson D. J. (2017). Independent core attenuation control in multicore fibers by direct femtosecond laser inscription. Optical Fiber Commun. Conf. (OFC2017), W3H.1.

[4] Yamashita Y., Matsui T., Sakamoto T., Aozasa S., Wada M., Mori T., and Nakajima K. (2020). Reduction of differential mode gain in a two-mode amplifier using a void-inscribed EDF. Appl. Opt., 59 (3), 9574-9580.

[5] Glezer E. N. and Mazur E. (1997). Ultrafast-laser driven micro-explosions in transparent materials. Appl. Phys. Lett., 71 (7), 882-884.

[6] Du D., Liu X., Korn G., Squier J., and Mourou G. (1994). Laser-induced breakdown by impact ionization in SiO_2 with pulse widths from 7 ns to 150 fs. Appl. Phys. Lett., 64 (23), 3071-3073.

[7] Stuart B. C., Feit M. D., Rubenchik A. M., Shore B. W., and Perry M. D. (1995). Laser-induced damage in dielectrics with nanosecond to subpicosecond pulses. Phys. Rev. Lett., 74 (12), 2248-2251.

[8] Stuart B. C., Feit M. D., Herman S., Rubenchik A. M., Shore B. W., and Perry M. D. (1996). Optical ablation by high-power short-pulse lasers. J. Opt. Soc. Am. B, 13 (2), 459-468.

[9] Stuart B. C., Feit M. D., Herman S., Rubenchik A. M., Shore B. W., and Perry M. D. (1996). Nanosecond-to-femtosecond laser-induced breakdown in dielectrics. Phys. Rev. B, 53 (4), 1749-1761.

[10] Von der Linde D. and Schüler H. (1996). Breakdown threshold and plasma formation in femtosecond laser-solid interaction. J. Opt. Soc. Am. B, 13 (1), 216-222.

[11] Lenzner M., Krüger J., Sartania S., Chen Z., Spielmann C., Mourou G., Kautek W., and Krausz F. (1998). Femtosecond optical breakdown in dielectrics. Phys. Rev. Lett., 80 (18), 4076-4079.

[12] Schaffer C. B., Brodeur A., and Mazur E. (2001). Laser-induced breakdown and damage in bulk transparent materials induced by tightly focused femtosecond laser pulses. Meas. Sci. Technol., 12, 1784-1794.

[13] Smith A. V. and Do B. T. (2008). Bulk and surface laser damage of silica by picosecond and nanosecond pulses at 1064 nm. Appl. Opt., 47 (26), 4812-4832.

[14] Smith A. V., Do B. T., Hadley G. R., and Farrow R. L. (2009). Optical damage limits to pulse energy from fibers. IEEE J. Selected Topics in Quantum Electron., 15 (1), 153-158.

[15] Davis K. M., Miura K., Sugimoto N., and Hirao K. (1996). Writing waveguides in glass with a femtosecond laser. Opt. Lett., 21 (21), 1729-1731.

[16] Miura K., Qiu J., Inouye H., Mitsuyu T., and Hirao K. (1997). Photowritten optical waveguides in various glasses with ultrashort pulse laser. Appl. Phys. Lett., 71 (23), 3329-3331.

[17] Schaffer C. B., Brodeur A., García J. F., and Mazur E. (2001). Micromachining bulk glass by use of femtosecond laser pulses with nanojoule energy. Opt. Lett., 26 (2), 93-95.

[18] Kanehira S., Si J., Qiu J., Fujita K., and Hirao K. (2005). Periodic nanovoid structures via femtosecond laser irradiation. Nano Lett., 5 (8), 1591-1595.

[19] Kanehira S., Miura K., Fujita K., and Hirao K. (2006). Nano-sized modification of transparent materials using femtosecond laser irradiation. Proc. Soc. Photo-Opt. Instrum. Eng., 6413, 6413M1-6413M9.

[20] Tzortzakis S., Sudrie L., Franco M., Prade B., Mysyrowicz A., Couairon A., and Bergé L. (2001). Self-guided propagation of ultrashort IR laser pulses in fused silica. Phys. Rev. Lett., 87 (21), 213902-1-213902-4.

[21] Sudrie L., Couairon A., Franco M., Lamouroux B., Prade B., Tzortzakis S., and Mysyrowicz A. (2002). Femtosecond laser-induced damage and filamentary propagation in fused silica. Phys. Rev. Lett., 89 (18), 18660-1-18660-4.

[22] Wu Z., Jiang H., Luo L., Guo H., Yang H., and Gong Q. (2002). Multiple foci and a long filament observed with focused femtosecond pulse propagation in fused silica. Opt. Lett., 27 (6), 448-450.

[23] Wu Z., Jiang H., Sun Q., Yang H., and Gong Q. (2003). Filamentation and temporal reshaping of a femtosecond pulse in fused silica. Phys. Rev. A, 68, 063820.

[24] Kashyap R. and Blow K. J. (1988). Observation of catastrophic self-propelled self-focusing in optical fibres. Electron. Lett., 24 (1), 47-49.

[25] Kashyap R. (1988). Self-propelled self-focusing damage in optical fibres. Lasers'87: Proc. Xth Int. Conf. Lasers and Applications, 859-866, STS Press, McLean.

[26] Hand D. P. and Russell P. St. J. (1988). Solitary thermal shock waves and optical damage in optical fibers: the fiber fuse. Opt. Lett., 13 (9), 767-769.

[27] Hand D. P., Townsend J. E., and Russell P. St. J. (1988). Optical damage in fibers: the fiber fuse. Proc. Conf. on Lasers and Electro-Optics (CLEO), WJ1.

[28] Hand D. P. and Russell P. St. J. (1988). Soliton-like thermal shock-waves in optical fibres: origin of periodic damage tracks. Proc. Eur. Conf. Opt. Commun., 111-114.

[29] Yoshioka M., Hidai H., and Tokura H. (2006). CW-laser induced modification in glasses by laser backside irradiation (LBI). Proc. Soc. Photo-Opt. Instrum. Eng., 6106, 61060Y-1-61060Y-9.

[30] Hidai H., Yoshioka M., Hiromatsu K., and Tokura H. (2009). Glass modification by continuous-wave laser backside irradiation (CW-LBI). Appl. Phys. A, 96, 869-872.

[31] Hidai H., Yoshioka M., Hiromatsu K., and Tokura H. (2010). Structual changes in silica glass by continuous-wave laser backside irradiation. J. Am. Ceram. Soc., 93 (3), 1597-1601.

[32] Itoh S., Hidai H., and Tokura H. (2013). Experimental and numerical study of mechanism of glass modification process by continuous-wave laser backside irradiation (CW-LBI). Appl. Phys. A, 112, 1043-1049.

[33] Tokunaga D., Sato S., Hidai H., Matsusaka S., Chiba A., and Morita N. (2019). A novel method of triggering fiber fuse inside glass by optical breakdown and glass drilling as its application. Appl. Phys. A, 125, 400.

[34] Shuto Y., Yanagi S., Asakawa S., Kobayashi M., and Nagase R. (2004). Fiber fuse phenomenon in step-index single-mode optical fibers. IEEE J. Quantum Electron., 40 (8), 1113-1121.

[35] Shuto Y. (2014). Heat conduction modeling of fiber fuse in single-mode optical fibers. J. Photonics, 2014, 645207.

[36] Shuto Y. (2015). Simulation of fiber fuse phenomenon in single-mode optical fibers. Advances in Optical Fiber Technology, Eds. Yasin M., Arof H., and Harun S. W., Chap. 5, 159-197, InTech, Rijeka.

[37] Shuto Y. (2010). Evaluation of high-temperature absorption coefficients of ionized gas plasmas in optical fibers. IEEE Photon. Technol. Lett., 22 (3), 134-136.

[38] Giuliano C. R. (1964). Laser-induced damage to transparent dielectric materials. Appl. Phys. Lett., 5 (7), 137-139.

[39] Fersman I. A. and Khazov K. D. (1970). Damage of transparent dielectric surfaces by a laser beam. Sov. Phys. Tech. Phys., 15, 834-838.

[40] Giuliano C. R. (1972). Laser-induced damage in transparent dielectrics: The relationship between surface damage and surface plasmas. IEEE J. Quantum Electron., QE-8 (9), 749-754.

[41] Crisp M. D., Boling N. L., and Dubé G. (1972). Importance of Fresnel reflections in laser surface damage of transparent dielectrics. Appl. Phys. Lett., 22 (8), 364-366.

[42] Boling N. L., Crisp M. D., and Dubé G. (1973). Laser induced surface damage. Appl. Opt., 12 (4), 650-660.

[43] Génin F. Y., Salleo A., Pistor T. V., and Chase L. L. (2001). Role of light intensification by cracks in optical breakdown on surfaces. J. Opt. Soc. Am. A, 18 (10), 2607-2616.

[44] Bloembergen N. (1974). Laser-induced electric breakdown in solids. IEEE J. Quantum Electron., QE-10 (3), 375-386.

[45] Bloembergen N. (1973). Role of cracks, pores, and absorbing inclusions on laser induced damage threshold at surfaces of transparent dielectrics. Appl. Opt., 12 (4), 661-664.

[46] Shuto Y. (2020). Cavity pattern formation and its dynamics of fiber fuse in single-mode optical fibers. J. Informatics Math. Sci., 12 (4), 271-288.

[47] Jensen B. (1985). The quantum extension of the Drude-Zener theory in polar semiconductors. Handbook of Optical Constants of Solids, Ed. Palik E. D., Chap. 9, Academic Press Inc., New York.

[48] Chemical Society of Japan. (1984). Chemical Data Book, 3rd Ed., Chap. 14, Maruzen, Tokyo.

[49] Shuto Y. (2016). End face damage and fiber fuse phenomenon in single-mode fiber-optic connectors. J. Photonics, 2016, 2781392.

[50] Davis D. D., Mettler S. C., and DiGiovani D. J. (1996). A comparative evaluation of fiber fuse models. Proc. Soc. Photo-Opt. Instrum. Eng., 2966, 592-606.

[51] Shibata N. and Edahiro T. (1982). Refractive-index dispersion for GeO_2-, P_2O_5- and B_2O_3-doped silica glasses in optical fibers. Trans. IECE Jpn., E65 (3), 166-172.

[52] Smith W. L. (1978). Laser-induced breakdown in optical materials. Opt. Eng. 17 (5), 489-503.